



## PREDICTION OF ENERGY-BASED INTENSITY MEASURES IN PERFORMANCE-BASED EARTHQUAKE ENGINEERING

Fabrizio MOLLAIOLI<sup>1</sup>, Yin CHENG<sup>2</sup>, Andrea LUCCHINI<sup>3</sup>,

### ABSTRACT

In recent years some energy-based parameters have been paid more attention and indicated as potential intensity measures for predicting the structural seismic demand in the framework of Performance-Based Earthquake Engineering (PBEE). Two representatives of those parameters are relative and absolute elastic input energy. In order to apply these two intensity measures into practical application in PBEE. Two efforts have been made in this study. Firstly, new improved ground motion prediction equations (GMPEs) was established for them by taking advantage of a large set of strong ground motions selected from the NGA database and considering the influence of more effects. Secondly, since these GMPEs only consider the marginal distribution of individual spectral values without giving any information about the joint distribution of the spectral values at different periods, we proposed new models for the prediction of the correlation coefficients of the energy-based spectral values at different periods or/and directions. In the end, some possible applications of the proposed models are discussed.

### INTRODUCTION

In Performance-Based Earthquake Engineering (PBEE), the ground motion intensity measure (IM), which quantifies the severity of a seismic event, is used as that parameter which defines the seismic hazard at a specified site. Several studies proposing energy-based concepts for the definition of the earthquake IM have been carried out in the past (e.g., Uang and Bertero 1990; Decanini and Mollaioli 1998, 2001; and the most recent Takewaki 2004; Kalkan and Kunnath 2008; Benavent-Climent et al. 2010a, b; Lucchini et al. 2011; Takewaki and Tsujimoto 2011; Mollaioli et al. 2011; Mollaioli et al. 2013; and Lopez-Almansa et al. 2013). Among the different energy-based parameters that have been studied, the relative and absolute elastic input energy and the corresponding equivalent velocities are those that more than others have been considered as potential measures of seismic demand in structures. The good prediction capabilities of these IMs are due to the fact that their values do not only depend on the amplitude, frequency content, and duration of the ground motion, but also on the dynamic properties of the structure. Moreover, energy-based methodologies appear more helpful in concept, as they permit a rational assessment of the energy absorption and dissipation mechanisms that can be effectively accomplished to balance the energy imparted to the structure. The objective of this

<sup>1</sup> Department of Structural and Geotechnical Engineering, Sapienza University of Rome, via Gramsci 53, 00197 Rome, Italy, [fabrizio.mollaioli@uniroma1.it](mailto:fabrizio.mollaioli@uniroma1.it)

<sup>2</sup> Department of Structural and Geotechnical Engineering, Sapienza University of Rome, via Gramsci 53, 00197 Rome, Italy, [andrea.lucchini@uniroma1.it](mailto:andrea.lucchini@uniroma1.it)

<sup>3</sup> Department of Structural and Geotechnical Engineering, Sapienza University of Rome, via Gramsci 53, 00197 Rome, Italy, [yin.cheng1983@gmail.com](mailto:yin.cheng1983@gmail.com)

study is to establish new ground motion prediction equations (GMPEs) for both the absolute and the relative elastic input energy equivalent velocity spectrum ( $V_{Ela}$  and  $V_{Elr}$ ). The equations will be derived using a large set of strong ground motions selected from the NGA database. Advances with respect to the GMPEs presently available in the literature will be obtained by accounting for the effects of both fault mechanism and soil condition. A random effects model for considering the variation of records within-event and between-events will be employed in the regression analyses for the development of the prediction equations. Moreover, as these GMPEs only consider the marginal distribution of individual spectral values without giving any information about the joint distribution of the spectral values at different periods, the second objective of this study is to propose models for the prediction of the correlation coefficients of the  $V_{Ela}$  and  $V_{Elr}$  spectral values. To this purpose, firstly, a dataset of correlation coefficients values was derived from a database of ground motions records. Then, functional forms of equations adopted in the literature to predict other IMs were calibrated to fit the  $V_{Ela}$  and  $V_{Elr}$  correlation coefficients data. Finally new predictive equations were developed in order to improve the fitness between the observed data and the predicted values. At the end of this study, some possible applications of the proposed equations are shown.

## ELASTIC INPUT ENERGY EQUIVALENT VELOCITIES

For a damped SDOF system subjected to ground acceleration  $\ddot{u}_g$ , the equation of motion can be written in the following two ways (Uang and Bertero, 1990):

$$m(\ddot{u}_g + \ddot{u}) + c\dot{u} + f_s = 0 \quad (1)$$

$$m\ddot{u} + c\dot{u} + f_s = -m\ddot{u}_g \quad (2)$$

where  $u$  is the relative displacement of the SDOF system with respect to the ground,  $u_g$  is the ground displacement,  $c$  is the viscous damping coefficient and  $f_s$  is the restoring force, and  $m$  is the mass.

Integrating Eqs. (1)-(2) with respect to  $u$ , and denoting with  $u_t$  the total displacement of the SDOF system ( $u_t = u + u_g$ ), we obtain the two following equations:

$$\frac{m\dot{u}_t^2}{2} + \int (c\dot{u})du + \int f_s du = \int m\ddot{u}_t du_g \quad (3.a)$$

$$\frac{m\dot{x}^2}{2} + \int (c\dot{x})dx + \int f_s dx = -\int m\ddot{x}_g dx \quad (3.b)$$

From Eqs. (3.a)-(4.b) two different input energies can be expressed (e.g., see Uang and Bertero 1990): the absolute input energy  $E_{Ia}$  (i.e.,  $\int m\ddot{u}_t du_g$  corresponding to the right side term of Eq. (3.a), and the relative input energy  $E_{Ir}$  (i.e.,  $-\int m\ddot{x}_g dx$  corresponding to the right side term of Eq. (3.b). Furthermore, these two energy parameters can be conveniently converted into equivalent velocities using the following equations:

$$V_{Ela} = \sqrt{2E_{Ia} / m} \quad (4)$$

$$V_{Elr} = \sqrt{2E_{Ir} / m} \quad (5)$$

Elastic  $V_{Ela}$  and  $V_{Elr}$  have been evaluated to derive the proposed GMPEs using a set of 1550 ground motion records from 63 main shock earthquakes, selected from the NGA database ([http://peer.berkeley.edu/peer\\_ground\\_motion\\_database/site](http://peer.berkeley.edu/peer_ground_motion_database/site)). Each record represents a free-field motion, characterized by a measured or estimated  $V_{s30}$ , obtained from earthquakes located within the shallow continental crust in a tectonically active region.

## GROUND MOTION PREDICTION EQUATIONS OF ELASTIC INPUT ENERGY EQUIVALENT VELOCITIES

In this paper a mixed-effects model was adopted to develop GMPEs (e.g., see Abrahamson and Youngs 1992; Özbey et al. 2004; Danciu and Tselentis 2007). The specific functional form used for the prediction of both  $V_{Ela}$  and  $V_{EIr}$  is:

$$\ln(IM) = a + b(M - 6) + c(M - 6)^2 + (d + fM) \ln \sqrt{R^2 + h^2} + e \ln(V_{s30} / 1130) + m1NR + m2RS \quad (6)$$

where

$IM$  is the considered IM ( $V_{Ela}$  or  $V_{EIr}$ );  $M$  is the moment magnitude;  $R$  is the closest distance to rupture;  $V_{s30}$  is the value of the average shear-wave velocity between 0 and 30 meters depth;  $a, b, c, d, e, f, m1, m2$  are the model coefficients; the focal depth  $h$  is used to provide a better fit to the data at short distances (Abrahamson and Silva 1997 ; Özbey et al. 2004). The variables NR and RS, used in order to account for fault mechanism effects, are given as follows:

$NR=1$  for normal fault mechanism and normal-oblique, 0 otherwise,

$RS=1$  for reverse fault and reverse-oblique mechanism, 0 otherwise,

$NR=0$  and  $RS=0$  for strike-slip fault mechanism.

Figs. 1-2 show the dependence of the inter-event and intra-event residuals on magnitude, distance and  $V_{S30}$  for  $V_{Ela}$ , correspondingly. For the case of  $V_{Ela}$  there is no significant trend or bias that results from the use of the considered functional form, confirming that the adopted function can be considered suitable for the selected predictor variables. The normal Quantile-Quantile plots for the residuals of  $V_{Ela}$ , reported in Fig. 3, show that both total and intra-event residuals, derived using the established GMPEs, have a very good fit to the assumed normal distribution. Comparable results were attained also for  $V_{EIr}$ .

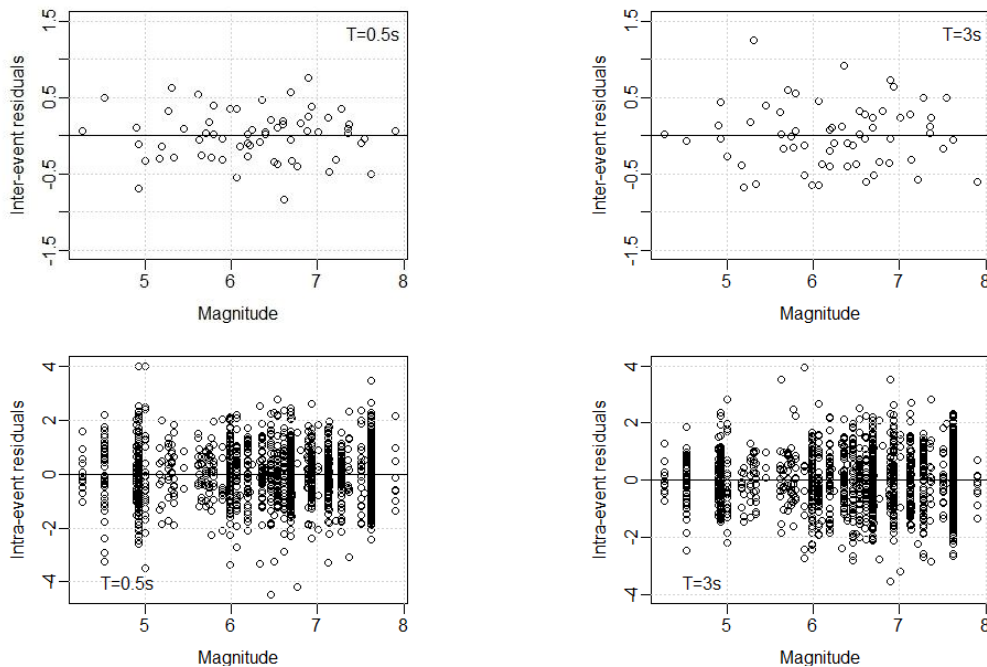


Fig. 1 Dependence of inter-event (upper panels) and intra-event (lower panels) residuals of  $V_{Ela}$  on moment magnitude.

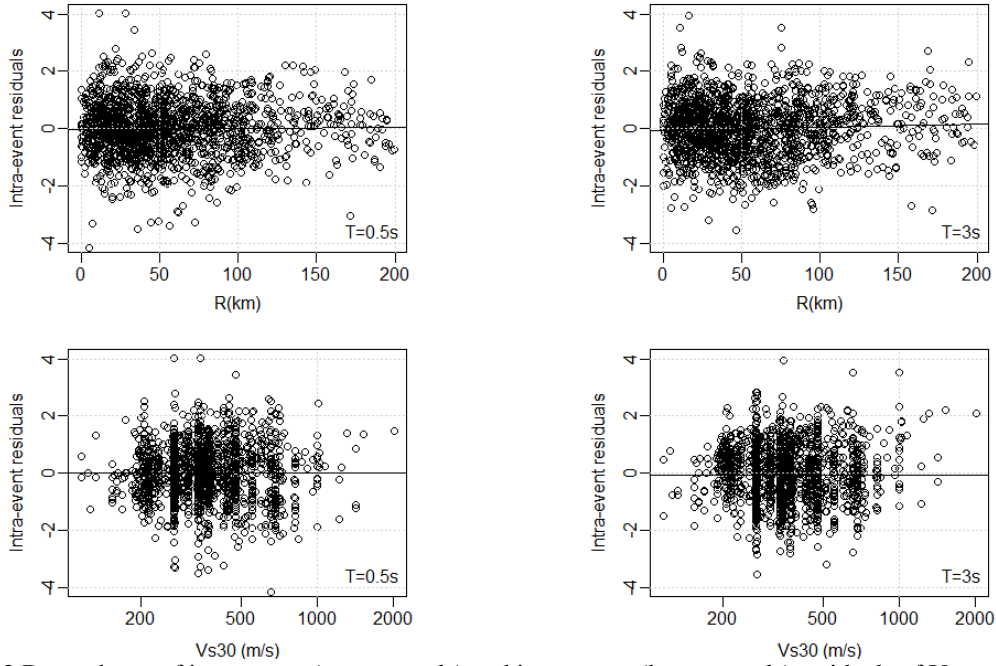


Fig. 2 Dependence of intra-event (upper panels) and intra-event (lower panels) residuals of  $V_{EIa}$  on rupture distance ( $R$ ).

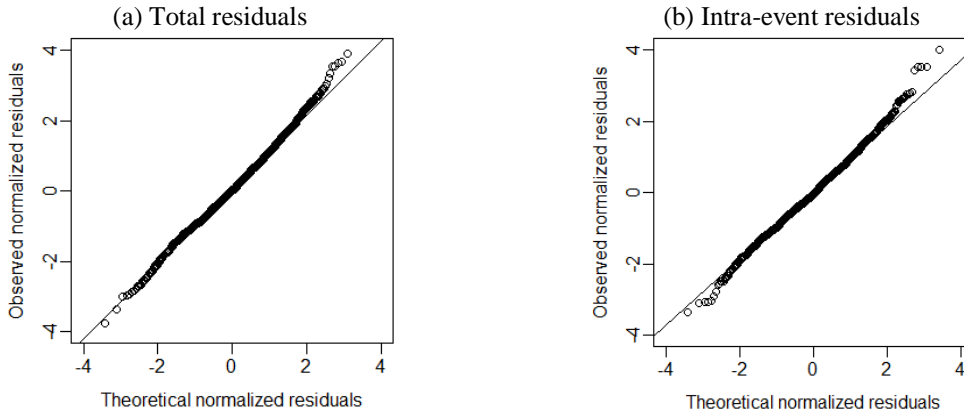


Fig. 3 Normal Q-Q plot of residuals obtained for  $V_{EIa}$  using the proposed GMPE.

In Fig. 4, the model coefficients of  $V_{EIa}$  and  $V_{EIr}$  computed at different period values  $T$  are related. It is shown that the linear and quadratic magnitude coefficients of the  $V_{EIa}$  and  $V_{EIr}$  functional forms at periods lower than around 1s are almost the same. This means that at short periods the scaling of the two velocities with magnitude is very comparable. A similar tendency can be also observed for the model coefficients  $m1$  and  $m2$  for period values lower than 1.5s, representing the same sensitivity of  $V_{EIa}$  and  $V_{EIr}$  on fault mechanism nature in this period range. At short periods, distance coefficients  $d$  and  $f$  of the two velocities are closely the same, but the  $h$  value is higher for  $V_{EIr}$  than for  $V_{EIa}$  indicating faster intensity attenuation for  $V_{EIr}$  than for  $V_{EIa}$ . Model coefficient  $e$  of  $V_{EIa}$  and  $V_{EIr}$  are very close independently from the period value, inferring that site effects for the two velocities are almost the same. Finally, opposite trends can be identified for standard errors in correspondence of  $T$  values lower and higher than 1s. Specifically, for  $T < 0.5s$  the values of  $\tau$  and  $\sigma$  obtained for  $V_{EIr}$  are significantly higher than those found for  $V_{EIa}$ . On the other hand, for  $T > 2s$  the values of the  $V_{EIa}$  standard errors are higher than those achieved in the  $V_{EIr}$  predictions.

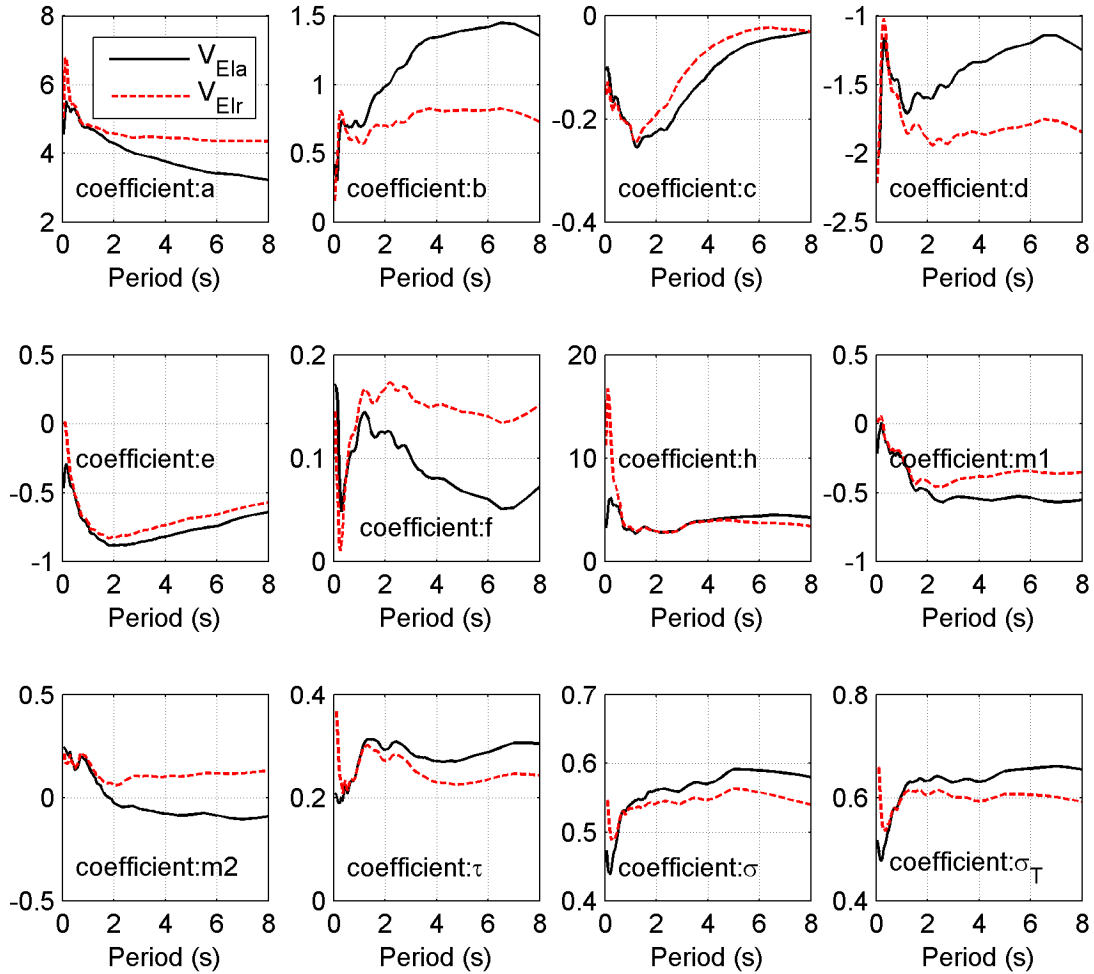


Fig. 4 Variation with period of the estimated model coefficients of the functional forms of  $V_{EIa}$  and  $V_{EIr}$

## PREDICTED $V_{EIa}$ AND $V_{EIr}$ SPECTRA

In Fig. 5,  $V_{EIa}$  and  $V_{EIr}$  spectra obtained with the proposed GMPEs for a strike-slip earthquake of 6.5 magnitude and a rupture distance equal to 30 km are illustrated. It is noteworthy to notice that while the intensity of  $V_{EIa}$  is always influenced by soil condition (highlighted by  $V_{s30}$  values),  $V_{EIr}$  does not depend on it at period values lower than 0.2s. In the same Figure, where a comparison between spectra produced by different types of fault mechanism is reported, it is shown that the two velocities show the same trend. For both of them, the intensity produced by an earthquake with a strike-slip fault mechanism ranges in between the intensities corresponding to normal and reverse-faulting earthquakes. In particular, the velocity values produced by strike-slip and normal fault earthquakes are pretty the same at short periods (lower than 0.2s), while at large periods (higher than about 1.5s), the velocity values produced by the strike-slip fault earthquake converge toward those of the reverse fault earthquake.

In Figs. 6-7 the two spectra of equivalent velocity are compared considering different distances and soil conditions, respectively. In this case, it can be detected that while at short periods (lower than about 0.2s) the dissimilarities between the  $V_{EIa}$  and  $V_{EIr}$  value is large, with the increase of magnitude at periods higher than 1s the difference reduces.

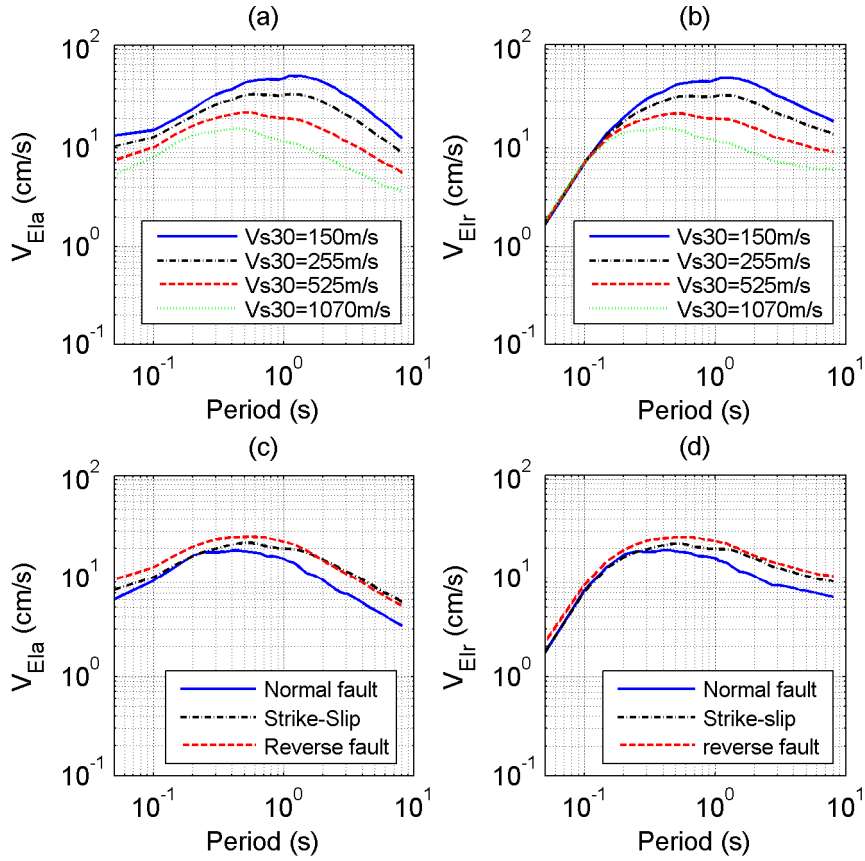


Fig. 5 Predicted  $V_{EIa}$  and  $V_{EIr}$  spectra for  $M=6.5$  and  $R=30$  km considering: different  $V_{s30}$  values (corresponding to different NEHRP soil conditions) for the same strike-slip fault mechanism (plots a and b), and different fault mechanisms for  $V_{s30}=525$  m/s (plots c and d).

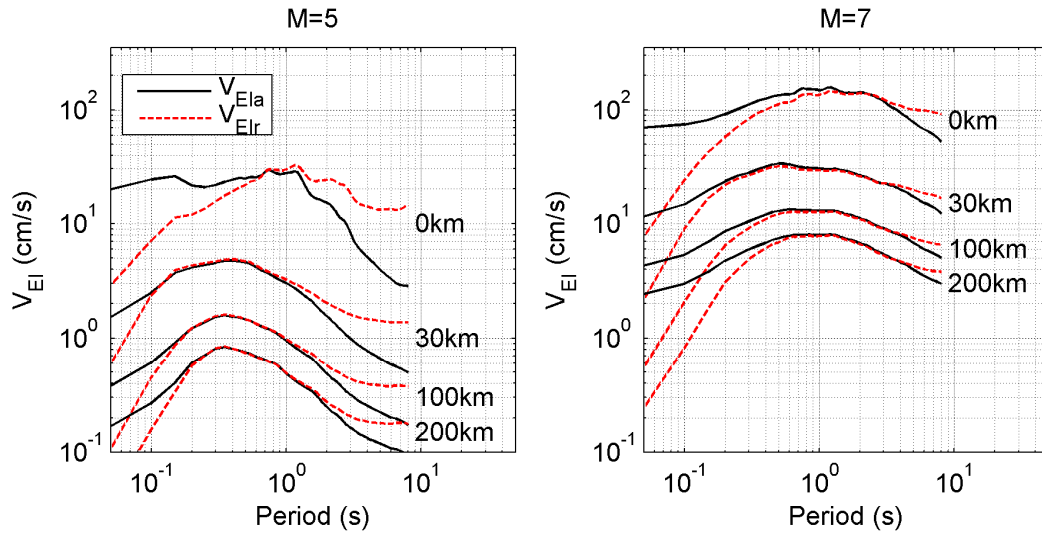


Fig. 6  $V_{EIa}$  and  $V_{EIr}$  spectra produced by a strike-slip earthquake, a  $V_{s30}$  equal to 525 m/s (corresponding to a soil type C, according to NEHRP classification), and various distance and magnitude values



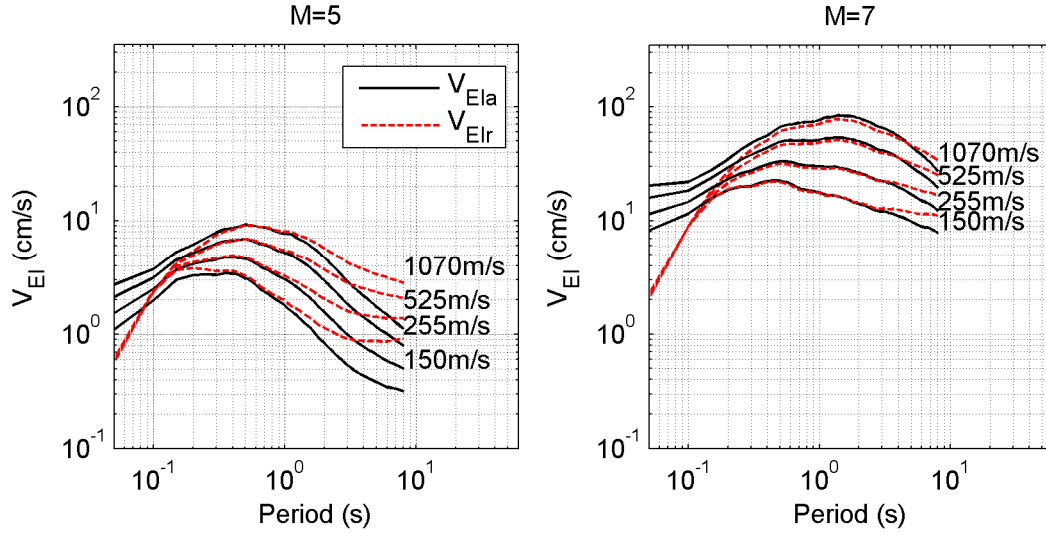


Fig. 7 Comparison between  $V_{EIa}$  and  $V_{EIr}$  spectra produced by a strike-slip earthquake, a distance equal to 30km, and various  $V_{s30}$  and magnitude values

### CORRELATION PREDICTIVE EQUATIONS FOR $V_{EIa}$ AND $V_{EIr}$

As already underlined, in order to give information about the joint distribution of the spectral values at different periods, new models for the prediction of the correlation coefficients of the  $V_{EIa}$  and  $V_{EIr}$  spectral values are proposed. Correlation coefficients are evaluated on the basis of the logarithm of input energy equivalent velocities of two horizontal components of each record:

$$\ln V_{EIx}(T) = f(M, R, T, \theta) + \sigma(T)\varepsilon_x(T) \quad \ln V_{EIy}(T) = f(M, R, T, \theta) + \sigma(T)\varepsilon_y(T) \quad (7)$$

where:  $V_{EI}$  represents observed values of  $V_{EIa}$  or  $V_{EIr}$  for each record considered in this study;  $x$  and  $y$  represent the two perpendicular horizontal components, respectively;  $f(M, R, T, \theta)$  is the predicted median of logarithmic  $V_{EIa}$  or  $V_{EIr}$  at a specific period  $T$ , evaluated through the GMPE that is a function of magnitude ( $M$ ), source to site distance ( $R$ ), period ( $T$ ) and other parameters ( $\theta$ );  $\sigma(T)$  is standard deviation of the predicted  $V_{EIa}$  or  $V_{EIr}$ , which is also provided by the GMPE.

The above two equations can also be simply modified so as to put in evidence the parameters  $\varepsilon_x(T)$  and  $\varepsilon_y(T)$  that account for the randomness of observation and follow the distribution with mean of zero and unit standard deviation:

$$\varepsilon_x(T) = \frac{\ln V_{EIx}(T) - f(M, R, T, \theta)}{\sigma(T)} \quad \varepsilon_y(T) = \frac{\ln V_{EIy}(T) - f(M, R, T, \theta)}{\sigma(T)} \quad (8)$$

Finally, the correlation of  $\varepsilon(T)$  can be estimated with the Eq. (9) using the Pearson product-moment correlation coefficient.

$$\rho_{\varepsilon(T_1), \varepsilon(T_2)} = \frac{\sum_{i=1}^n (\varepsilon_i(T_1) - \overline{\varepsilon(T_1)})(\varepsilon_i(T_2) - \overline{\varepsilon(T_2)})}{\sqrt{\sum_{i=1}^n (\varepsilon_i(T_1) - \overline{\varepsilon(T_1)})^2 \sum_{i=1}^n (\varepsilon_i(T_2) - \overline{\varepsilon(T_2)})^2}} \quad (9)$$

where:  $\varepsilon_i(T_1)$  and  $\varepsilon_i(T_2)$  are the  $i$ th observation of  $\varepsilon(T_1)$  and  $\varepsilon(T_2)$ ;  $n$  is the number of observation of  $\varepsilon$  at period  $T$ ;  $\overline{\varepsilon(T_1)}$  and  $\overline{\varepsilon(T_2)}$  are sample means of all  $n$  observations at  $T_1$  and  $T_2$ , respectively.

The correlation of  $\varepsilon(T)$  can be classified into three cases: the correlation coefficient of  $\varepsilon(T)$  for the different periods but the same horizontal component, noted as  $\rho_{\varepsilon(T_1),\varepsilon(T_2)}$ ; the correlation coefficient for the same period but different horizontal orthogonal components, noted as  $\rho_{\varepsilon_x(T),\varepsilon_y(T)}$ ; the correlation coefficient for the different periods and different horizontal orthogonal components, noted as  $\rho_{\varepsilon_x(T_1),\varepsilon_y(T_2)}$ . The Fig. 8 show the contours of the correlation coefficients versus  $T_1$  and  $T_2$ , while the Fig. 9 present the change of correlation coefficients as a function of  $T_1$  for a set of periods  $T_2$ .

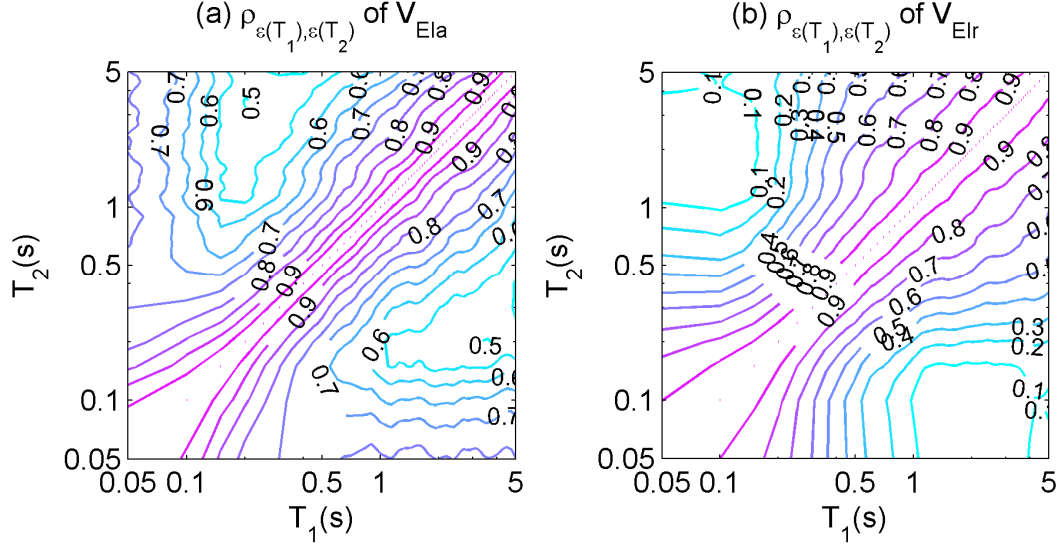


Fig. 8 Contours of empirical horizontal correlation coefficients of (a) absolute input energy equivalent velocity ( $V_{EIa}$ ) spectral values and (b) relative input energy equivalent velocity ( $V_{EIr}$ ) spectral values for  $T_1$  and  $T_2$

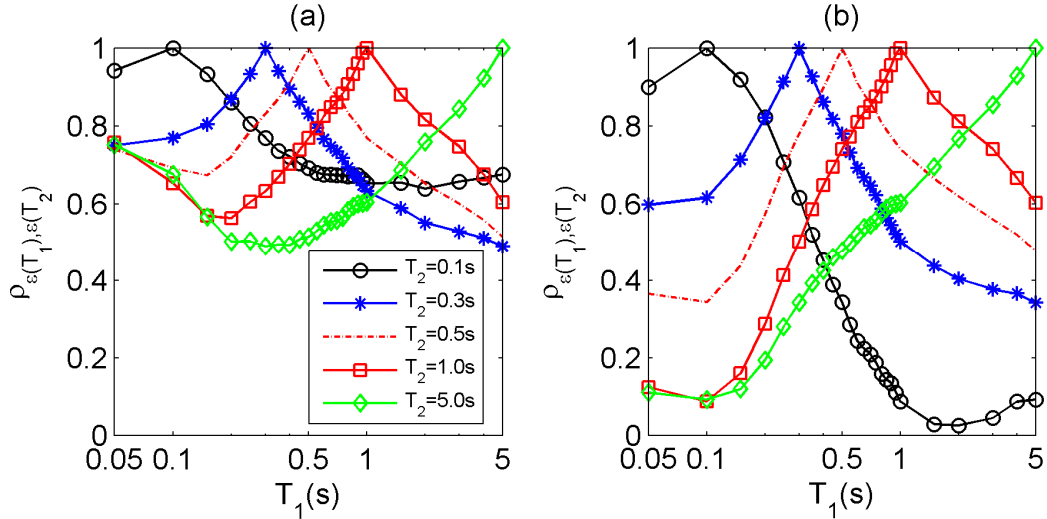


Fig. 9 Empirical horizontal coefficients of (a)  $V_{EIa}$  and (b)  $V_{EIr}$  spectral values versus  $T_1$ , for variable  $T_2$  values, calculated by using the proposed GMPEs

By comparing among Figs. 8 and 9, it is shown that the correlation coefficient values related to  $V_{EIa}$  is larger than  $V_{EIr}$ . In other words,  $V_{EIa}$  values in the same component at different periods are more correlated than  $V_{EIr}$ .

In this research, for fitting the correlations coefficients with an analytic equation, we adopted the same nonlinear regression method as that used by Baker and Cornell (2006). With this procedure, Fisher z transformation (Neter et al. 1996) is firstly applied to correlation coefficients, and simple least-squares regression is utilized to these z values (see Baker and Cornell 2006 and Baker and Jayaram 2008).



In the present study three different functional forms were used to develop the correlation equations: two selected from the literature, namely, those proposed by Baker and Cornell (2006) and Cimellaro (2013), and a new proposal.

The predictive model of correlation coefficients proposed by Backer and Cornell (2006) considers the following relationship:

$$\rho_{\varepsilon(T_1),\varepsilon(T_2)} = 1 - \cos\left(\frac{\pi}{2} - (A0 - A1 \cdot I_{(T_{\min} < A2)} \ln\left(\frac{T_{\min}}{A2}\right)) \ln\left(\frac{T_{\max}}{T_{\min}}\right)\right) \quad (10)$$

where  $T_{\min} = \min(T_1, T_2)$ ;  $T_{\max} = \max(T_1, T_2)$ ;  $I_{(T_{\min} < A2)}$  is an indicator function equal to 1 if  $T_{\min} < A2$  and equal to 0 otherwise. The contour of the observed and predicted correlation coefficients are plotted in Fig. 10(a)-(b).

Cimellaro (2013) proposed a model of correlation coefficients of  $S_a$  for the same horizontal or vertical component at two different periods without indicator function. This equation provides improved predictive models of correlation of  $S_a$  for earthquakes in Europe. The predictive model of correlation coefficients is represented by

$$\rho_{\varepsilon(T_1),\varepsilon(T_2)} = 1 - \left( \frac{a + b \ln(T_{\min}) + c(\ln(T_{\max}))^2}{1 + d \ln(T_{\max}) + e(\ln(T_{\min}))^2} \right) \ln\left(\frac{T_{\min}}{T_{\max}}\right) \quad (11)$$

In Eq. (11),  $T_{\min} = \min(T_1, T_2)$  and  $T_{\max} = \max(T_1, T_2)$ ,  $T_1$  and  $T_2$  are different periods in a single component. After fitting the observed correlation coefficients of  $V_{Ela}$  and  $V_{Elr}$  with this model, the parameters of this model are evaluated and the predicted correlation coefficients with the corresponding observed coefficients are shown in Fig. 10(c)-(d).

The predicted correlation coefficients of  $V_{Ela}$  and  $V_{Elr}$  by the model of Backer and Cornell (2006) do not match well the corresponding observed values (Fig. 10). On the other hand, the model of Cimellaro (2013) better fit the observed correlation coefficients than the model of Backer and Cornell (2006). Finally, in order to improve the robustness of the model, a new predictive model of correlation coefficients of  $V_{Ela}$  and  $V_{Elr}$ , given by following two equations, is proposed and the results are shown in Fig. 10(e,f):

$$\rho_{\varepsilon(T_1),\varepsilon(T_2)} = 1 - \cos\left(\frac{\pi}{2} - (B1 - A1 \cdot I_{(T_{\min} < A2)} \ln\left(\frac{T_{\min}}{A2}\right)) \ln\left(\frac{T_{\max}}{T_{\min}}\right)\right) \quad (12)$$

$$B1 = - \frac{a + b \ln(T_{\min}) + c(\ln(T_{\max}))^2}{1 + d \ln(T_{\max}) + e(\ln(T_{\min}))^2} \quad (13)$$

where  $I_{(T_{\min} < A2)}$  equal to 1 when  $T_{\min} < A2$  and equal to 0 otherwise. This model is proposed by incorporate the model of Baker and Cornell (2006) with the one of Cimellaro (2013).  $B1$  expressed in Eq. (13) has the same form as a part of model of Cimellaro (2013) expressed in Eq. (11). The proposed model will become the same model as that of Cimellaro (2013) when  $T_{\min} > A2$ . Conversely, when  $T_{\min} < A2$  the proposed model will have the same form as the model of Backer and Cornell (2006).

## CONCLUSIONS

The prediction of the structural seismic response by the absolute input energy equivalent velocity  $V_{Ela}$  and the relative input energy equivalent velocity  $V_{Elr}$  can be considered in some cases as good alternatives with respect to common intensity measures ( e.g., peak ground acceleration or the pseudo-spectral acceleration ) used in performance-based earthquake engineering.

In the present paper, a new proposal of empirical ground motion prediction equations developed on the basis of a mixed-effect model for estimating both  $V_{Ela}$  and  $V_{Elr}$ , is illustrated. The proposed

relationships can be applied to estimate  $V_{Ela}$  and  $V_{Elr}$  for shallow crustal earthquakes occurring in active tectonic region, with a magnitude range of 5 to 8, a distance less than 200 km, and a  $V_{s30}$  value in the range of 150-1500m/s.

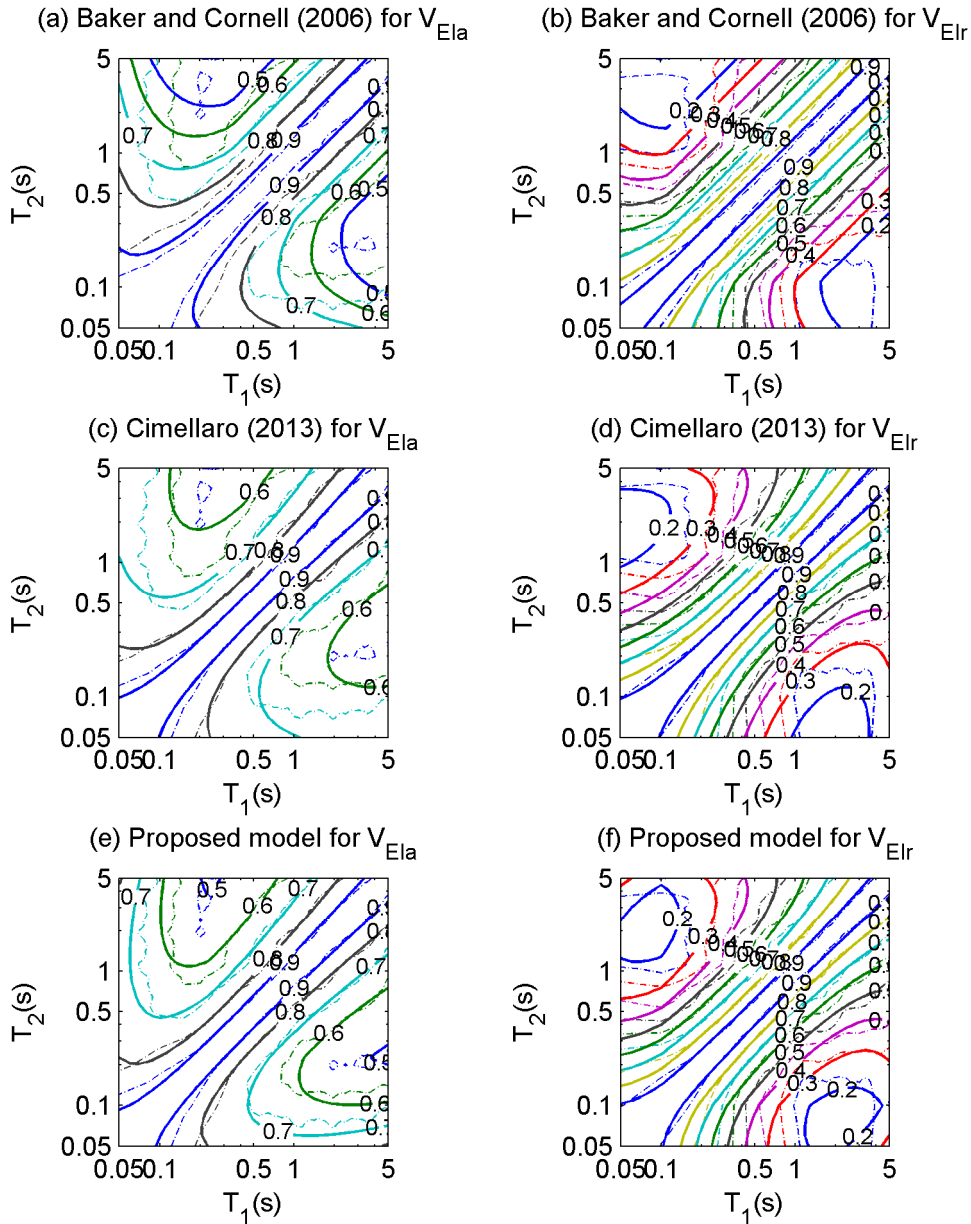


Fig. 10 Contour of observed (dash-dot lines) and predicted (solid lines) correlation coefficients of  $V_{Ela}$  and  $V_{Elr}$  at two periods ( $T_1$  and  $T_2$ ) in the same component

The enhancements with respect to existing prediction equations for input energy equivalent velocity spectra can be recognized in the following: the proposed equations have been developed using a large number of records characterized by a wide range of magnitude and distance; they include a  $V_{s30}$  term that enables a better evaluation of soil conditions effects; they also incorporate terms to explicitly account for different types of fault mechanisms; a prediction equation for the relative input energy equivalent velocity has been also proposed.

In the second part of the paper the predictions of the correlation between the spectral values of above mentioned two energy-based earthquake intensity measures have been evaluated with a newly suggested model. Three distinctive case studies of correlation were examined for both  $V_{Ela}$  and  $V_{Elr}$ : the correlation between the two ordinates of the equivalent velocity spectrum of the single horizontal

component of the ground motion; the correlation between the ordinates of the spectra of the two perpendicular horizontal components calculated at the same period value; the correlation between the ordinates of the spectra of the two perpendicular horizontal components calculated at two different periods.

The reason of such kind of research is that the proposed predictive relations for the correlation coefficients of  $V_{Ela}$  and  $V_{Elr}$  are a useful tool that can be applied in seismic hazard analysis problems or ground motion selection and modification methods. By using them, for example, the conditional mean spectrum of  $V_{Ela}$  and  $V_{Elr}$  can be easily computed, and energy-related scalar intensity measures derived from  $V_{Ela}$  and  $V_{Elr}$  (as shown in Mollaioli et al. 2013) can be predicted. Obviously, it is important to note that these models are strictly empirical, and thus, their use should not be extrapolated beyond the range over which the observed values were fit.

## ACKNOWLEDGMENTS

The financial support of both the Italian Ministry of the Instruction, University and Research (MIUR) and the Italian Network of University Laboratories of Seismic Engineering (ReLUIS) is gratefully acknowledged.

## REFERENCES

- Abrahamson, N.A., Youngs, R.R. (1992), "A stable algorithm for regression analyses using the random effects model", *Bull. Seismol. Soc. Am.*, 82(1), 505–510.
- Benavent-Climent, A., Lopez-Almansa, F., Bravo-Gonzalez, D.A. (2010a), "Design energy input spectra for moderate-to-high seismicity regions based on Colombian earthquakes", *Soil. Dyn. Earthq. Eng.*, 30(11), 1129–1148.
- Benavent-Climent, A., Zahran R. (2010b), "Seismic evaluation of existing RC frames with wide beams using an energy-based approach", *Earthquakes and Structures*, 1(1), 93–108.
- Baker, J. and Cornell, C.A. (2006), "Correlation of response spectral values for multicomponent ground motions", *Bull. Seismol. Soc. Am.*, 96(1), 215–227.
- Baker, J. and Jayaram, N. (2008), "Correlation of spectral acceleration values from NGA ground motion models", *Earthq. Spectra*, 24(1), 299–317.
- Chapman, M.C. (1999), "On the use of elastic input energy for seismic hazard analysis", *Earthq. Spectra*, 15(4), 607–635.
- Cimellaro, G.P. (2013), "Correlation in spectral acceleration for earthquakes in Europe", *Earthq. Eng. Struct. Dyn.*, 42(4), 623–633.
- Danciu, L., Tselentis, G.A. (2007), "Engineering ground-motion parameters attenuation relationships for Greece", *Bull. Seismol. Soc. Am.*, 97(1), 162–183.
- Decanini, L., Mollaioli, F. (1998), "Formulation of elastic earthquake input energy spectra", *Earthq. Eng. Struct. Dyn.*, 27(13), 1503–1522.
- Decanini, L., Mollaioli, F. (2001), "An energy-based methodology for the assessment of seismic demand", *Soil. Dyn. Earthq. Eng.*, 21(2), 113–137.
- Kalkan, E., Kunnath, S.K. (2008), "Relevance of absolute and relative energy content in seismic evaluation of structures", *Adv. Struct. Eng.*, 11(1), 17–34.
- López-Almansa, F., Yazgan, A., Benavent-Climent, A. (2013), "Design energy input spectra for high seismicity regions based on Turkish registers", *Bull. Earthq. Eng.*, 11(4), 885–912.
- Lucchini, A., Mollaioli, F., Monti, G. (2011), "Intensity measures for response prediction of a torsional building subjected to bi-directional earthquake ground motion", *Bull. Earthq. Eng.*, 9(5), 1499–1518.
- Mollaioli, F., Bruno, S., Decanini, L., Saragoni, R. (2011), "Correlations between energy and displacement demands for performance-based seismic engineering", *Pure Appl. Geophys.*, 168(1-2), 237–259.
- Mollaioli, F., Lucchini, A., Cheng, Y., Monti, G. (2013), "Intensity measures for the seismic response prediction of base-isolated buildings", *Bull. Earthq. Eng.*, 11(5), 1841–1866.
- Neter, J., Kutner, M.H., Nachtsheim, C.J., Wasserman, W. (1996), "Applied linear statistical models", MacGraw-Hill, Boston, Massachusetts, USA
- Ozbey, C., Sari, A., Manuel, L., Erdik, M., Fahjan, Y. (2004), "An empirical attenuation relationship for northwestern Turkey ground motion using a random effects approach", *Soil. Dyn. Earthq. Eng.*, 24(2), 115–125.

- Takewaki, I. (2004), "Bound of Earthquake Input Energy", *Journal of Structural Engineering*, 130(9), 1289–1297.
- Takewaki, I., Tsujimoto, H. (2011), "Scaling of design earthquake ground motions for tall buildings based on drift and input energy demands", *Earthquakes and Structures*, 2(2), 171-187.
- Uang, C.M., Bertero, V.V. (1990), "Evaluation of seismic energy in structures", *Earthq. Eng. Struct. Dyn.*, 19(1), 77–90.